Error representation of the time-marching DPG scheme

Judit Muñoz-Matute[a,b], Leszek Demkowicz[b], David Pardo[c,a,d]

[a] *Basque Center for Applied Mathematics, Bilbao (BCAM), Spain*
[b] *Oden Institute for Computational Engineering and Sciences, The University of Texas at Austin, Austin, USA*
[c] *University of the Basque Country (UPV/EHU), Leioa, Spain*
[d] *IKERBASQUE, Basque Foundation for Science, Bilbao, Spain*

Abstract

In this article, we introduce an error representation function to perform adaptivity in time of the recently developed time-marching Discontinuous Petrov-Galerkin (DPG) scheme. We first provide an analytical expression for the error that is the Riesz representation of the residual. Then, we approximate the error by enriching the test space in such a way that it contains the optimal test functions. The local error contributions can be efficiently computed by adding a few equations to the time-marching scheme. We analyze the quality of such approximation by constructing a Fortin operator and providing an *a posteriori* error estimate. The time-marching scheme proposed in this article provides an optimal solution along with a set of efficient and reliable local error contributions to perform adaptivity. We validate our method for both parabolic and hyperbolic problems.

Keywords: DPG method, Error representation, Ultraweak formulation, Optimal test functions, Exponential integrators, Fortin operator

1. Introduction

The Discontinuous Petrov-Galerkin (DPG) method with optimal test functions is a well established method [10, 11] to approximate the solution of Partial Differential Equations (PDEs) proposed by Prof. Demkowicz and Gopalakrishnan about a decade ago [7, 9]. The principal idea is to construct optimal test functions in such a way that the discrete stability of the method is guaranteed. It has been applied in many frameworks [1, 4, 5, 8, 13, 16, 26]. It is well known that the DPG method can be interpreted as a minimum residual method and also as a mixed problem. In the latter, selecting an enriched test space, the method delivers a stable solution and a built-in error representation usually employed to perform adaptivity [6, 12, 15, 35].

There are previous articles about applying the DPG ideas to time-dependent problems. In [14, 18, 19, 25], the authors apply the DPG method in the space-time domain, enabling local space-time refinements. Conversely, authors in [21, 22, 36] apply and analyze the DPG method in space together with different time-stepping schemes for parabolic problems. In other works like [23, 37–39], the authors employ DPG-related ideas for solving both

transient and frequency-domain problems, employing minimum residual methods or the corresponding mixed problems.

Recently, in [32, 33], we developed a time-marching scheme based on the DPG method for transient parabolic and hyperbolic problems, respectively. The main idea of the method is to apply the DPG technology only in the time variable to the system of Ordinary Differential Equations (ODEs) obtained after semidiscretizing in space a PDE with a Bubnov-Galerkin method. For that, we first consider a broken ultraweak variational formulation of the problem where, in the hyperbolic case, we reduce it first to a first order system. Then, the selection of the adjoint norm in the test space allows us to compute the optimal test functions analytically as we are considering a 1D problem. We found that the optimal test functions corresponding to piecewise polynomials for the trial space are exponentials of the stiffness matrix coming from the space discretization. We proved that the equation to compute the trace variables is equivalent to Exponential Integrators [28–30]. Moreover, the solution in the element interiors delivers an L^2-projection of the exact solution. In order to employ the existing software [27] available to compute exponential-related functions, we relate the optimal test functions to the so-called $\varphi-$functions employed in exponential time-integrators. Summarizing, we developed a time-marching scheme that is an exponential integrator for the traces and, additionally, we can compute the element interiors.

In this work, we present an error representation that we employ to perform adaptivity in time for the time-marching DPG scheme we introduced in [32, 33]. We know from the DPG community that the DPG solution minimizes the residual of the problem in the dual norm. It is well known that the built-in error representation function in DPG is the Riesz representation of the residual [10]. Here, as we are considering a 1D problem, we can also compute this error representation function analytically. We give an explicit expression of the error for any discrete solution in the trial space as well as for the optimal solution delivered by the DPG time-marching scheme. However, these expressions are given in integral form and their use requires a suitable study of appropriate quadrature rules.

Instead, we adopt the so-called *practical DPG* [24] philosophy and we approximate the error representation function by enriching the test space. By doing so, we can compute the local error contributions as we solve the problem in the time-marching scheme by adding a few equations to the system. We construct a global Fortin operator, which is an orthogonal projection, and a-posteriori error estimation similar to [3] to prove that our approximation to the analytical error is reliable and efficient. We emphasize that we enrich the test space in such a way that it contains the analytical optimal test functions. Therefore, the time-marching scheme delivers the optimal solution and an approximation of the error. For that reason, we employ the Fortin constant for the *a posteriori* error estimation only and in this case, it does not affect the stability of the solution. We employ the local contributions of this approximated error to perform adaptivity in time via the Dörfler marking strategy [17]. We validate our adaptive method in both parabolic and hyperbolic problems.

This article is organized as follows: Section 2 presents the model problem and summarizes the time-marching scheme we developed in [32, 33]. In Section 3 we show the analytical error representation function for any discrete ansatz solution on the discrete trial space and,

in particular, for the optimal solution obtained with our time-marching scheme. Section 4 introduces a practical error representation function for the solution of the DPG method that we employ for adaptivity. Section 5 analyzes the approximation of the practical error to the analytical one by constructing a Fortin operator and developing an a posteriori error estimate. Section 6 presents numerical results of performing time adaptivity for both parabolic and hyperbolic problems. Finally, in Section 7, we summarize the conclusions and future work.

2. Time-marching DPG scheme

This section overviews the time-marching DPG scheme we introduced in [33] for parabolic problems. For simplicity, we consider a single Ordinary Differential Equation (ODE). The generalizations to hyperbolic problems and to systems of ODEs coming from the semidiscretization in space by the Bubnov-Galerkin method of Partial Differential Equations (PDEs) are summarized in [32, 33].

2.1. Model problem and variational setting

Let $I = (0, 1] \subset \mathbb{R}$. We consider the following first order ODE

$$\begin{cases} u' + \lambda u = f \quad \text{in } I, \\ u(0) = u_0, \end{cases} \tag{1}$$

where $\lambda \in \mathbb{R}\backslash\{0\}$, $u_0 \in \mathbb{R}$ and $f \in L^2(I)$ are given data.

We define a partition I_h of I as

$$0 = t_0 < t_1 < \ldots < t_{m-1} < t_m = 1,$$

where $I_k = (t_{k-1}, t_k)$ and $h_k = t_k - t_{k-1}$, $\forall\ k = 1, \ldots, m$. Related to this partition, we introduce the following trial and test (broken) spaces

$$\begin{aligned} U =& U^0 \times \hat{U} = L^2(I) \times \mathbb{R}^m, \\ V =& H^1(I_h) = \{v \in L^2(I) \mid v_{|_{I_k}} \in H^1(I_k),\ \forall\ I_k \in I_h\}. \end{aligned} \tag{2}$$

We define the jumps of a function $v \in V$ at each time t_k as

$$\begin{aligned} &[v]_k = v(t_k^+) - v(t_k^-), \ \ \forall\ k = 1, \ldots, m-1, \\ &[v]_m = -v(t_m^-), \end{aligned} \tag{3}$$

where $v(t_k^{\pm}) := \lim_{\varepsilon \to 0^+} v(t_k \pm \varepsilon)$. We consider an ultraweak variation formulation of (1) that reads

$$\begin{cases} \text{Find } z = (u, \hat{u}^1, \ldots, \hat{u}^m) \in U \text{ such that} \\ b(z, v) = l(v), \ \ \forall\ v \in V, \end{cases} \tag{4}$$

where

$$
\begin{aligned}
b(z,v) &:= \sum_{k=1}^{m} \int_{I_k} u(-v' + \lambda v) dt - \hat{u}^k [v]_k, \\
l(v) &:= \sum_{k=1}^{m} \int_{I_k} fv \; dt + u_0 v(0^+).
\end{aligned}
\tag{5}
$$

Finally, we consider the following trial and test norms

$$
\begin{aligned}
||z||_U^2 &= ||u||^2 + \sum_{k=1}^{m} |\hat{u}^k|^2, \\
||v||_V^2 &= \sum_{k=1}^{m} \int_{I_k} |-v' + \lambda v|^2 dt + [v]_k^2.
\end{aligned}
\tag{6}
$$

2.2. Optimal test spaces and discrete scheme

We select a discrete trial space $U_{h,p} = U_{h,p}^0 \times \hat{U} \subset U$, where $U_{h,p}^0$ is composed of piecewise polynomials of order p. We define an element $z_h = (u_h, \hat{u}_h^1, \ldots, \hat{u}_h^m) \in U_{h,p}$ (see Figure 1) where

$$
u_h^k(t) := u_h(t)_{|_{I_k}} = \sum_{i=0}^{p} u_{h,i}^k \left(\frac{t - t_{k-1}}{h_k} \right)^i.
$$

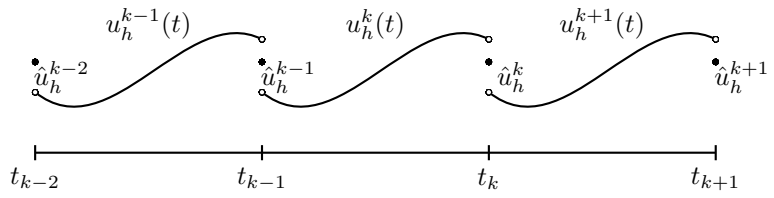

Figure 1: Approximated solution.

We define the optimal test space $V_{h,p}^{opt} \subset V$ corresponding to the trial space $U_{h,p}$ by the span of the functions solving the following problem: Given $z_h \in U_{h,p}$

$$
\begin{cases}
\text{Find } v \in V \text{ such that} \\
(v, \delta v)_V = b(z_h, \delta v), \;\; \forall \, \delta v \in V,
\end{cases}
\tag{7}
$$

where $(\cdot, \cdot)_V$ is the inner product corresponding to the adjoint test norm defined in (6). We proved in [33] that

$$
V_{h,p}^{opt} = span\{\hat{v}^k, v_j^k, \; \forall \; j = 0, \ldots, p, \; \forall \; k = 1, \ldots, m\},
$$

where the optimal test functions can be defined recursively as

$$\begin{aligned}
&\hat{v}^k(t) = e^{\lambda(t-t_k)}, \ \ \forall\, t \in I_k, \\
&v_j^k(t) = \frac{1}{\lambda}\left(\left(\frac{t-t_{k-1}}{h_k}\right)^j + \frac{j}{h_k} v_{j-1}^k(t) - \hat{v}^k(t)\right), \ \ \forall\, t \in I_k.
\end{aligned} \tag{8}$$

Moreover, the optimal test functions satisfy the adjoint equation

$$\begin{cases}
-(\hat{v}^k)' + \lambda \hat{v}^k = 0, \quad \hat{v}^k(t_k) = 1, \\
-(v_j^k)' + \lambda v_j^k = \left(\dfrac{t-t_{k-1}}{h_k}\right)^j, \quad v_j^k(t_k) = 0, \ \forall\, j = 0, \ldots, p.
\end{cases} \tag{9}$$

Finally, we solve

$$\begin{cases}
\text{Find } z_h = (u_h, \hat{u}_h^1, \ldots, \hat{u}_h^m) \in U_{h,p} \text{ such that} \\
b(z_h, v_h) = l(v_h), \ \ \forall\, v_h \in V_{h,p}^{opt},
\end{cases} \tag{10}$$

and we obtain the following equivalent DPG-based time-marching scheme $\forall\, k = 1, \ldots, m$

$$\begin{cases}
\hat{u}_h^k = \hat{u}_h^{k-1}\hat{v}^k(t_{k-1}) + \displaystyle\int_{I_k} f\hat{v}^k dt, \\
\displaystyle\sum_{i=0}^{p} u_{h,i}^k \frac{h_k}{i+j+1} = \hat{u}_h^{k-1} v_j^k(t_{k-1}) + \int_{I_k} f v_j^k dt, \ \forall\, j = 0, \ldots, p,
\end{cases} \tag{11}$$

where $\hat{u}_h^0 = u_0$.

3. Analytical error representation

It is well known in the DPG community [10] that the DPG method delivers an error representation function $\psi \in V$ whose norm equals the energy norm of the error of the solution, i.e.,

$$||z - z_h||_E = ||\psi||_V, \tag{12}$$

where the energy norm is defined as $||z||_E := \sup_{0 \neq v \in V} \dfrac{|b(z,v)|}{||v||_V}$. The function ψ is called the *error representation function* and it can be employed to perform adaptivity. It is defined as the solution of the following problem: Given $z_h \in U_{h,p}$

$$\begin{cases}
\text{Find } \psi \in V \text{ such that} \\
(\psi, \delta v)_V = b(z_h, \delta v) - l(\delta v), \ \ \forall\, \delta v \in V.
\end{cases} \tag{13}$$

Function ψ is thus the Riesz representation of the residual. Definition (13) holds for any approximation $z_h \in U_{h,p}$, including the optimal solution given in (10). For simplicity in the notation, we employ z_h in both cases specifying if it is the optimal solution of (10) or a perturbation of it. Similarly to problem (7), we can solve (13) analytically.

Proposition 1. *The error representation function (13) for any $z_h \in U_{h,p}$ with the variational setting defined in Section 2 is $\forall\ k = 1, \ldots, m$*

$$\psi^k(t) := \psi(t)_{|_{I_k}} = C_1^k e^{\lambda t} + C_2^k e^{-\lambda t} + \frac{e^{\lambda t}}{2\lambda}\int_t^{t_k} e^{-\lambda s} R^k(s)ds - \frac{e^{-\lambda t}}{2\lambda}\int_t^{t_k} e^{\lambda s} R^k(s)ds, \quad (14)$$

where $R^k(t) := (u_h^k(t))' + \lambda u_h^k(t) - f(t)_{|_{I_k}}$ is the residual at I_k and constants C_1^k and C_2^k are defined recursively as

$$\begin{cases} \quad C_2^1 = I_2^1 + \dfrac{e^{\lambda t_0}}{2\lambda} S_+^0, \\ C_2^{k+1} = I_2^{k+1} + C_2^k + \dfrac{e^{\lambda t_k}}{2\lambda}[u_h]_k, \ \ \forall\ k = 1, \ldots, m-1, \end{cases} \quad (15)$$

$$\begin{cases} C_1^m = (2\lambda - 1)C_2^m e^{-2\lambda t_m} + e^{-\lambda t_m} S_-^m, \\ C_1^k = C_1^{k+1} + I_1^{k+1} + 2\lambda C_2^k e^{-2\lambda t_k} + \dfrac{e^{-\lambda t_k}}{2\lambda}[u_h]_k + e^{-\lambda t_k} S_-^k, \ \ \forall\ k = m-1, \ldots, 1. \end{cases} \quad (16)$$

Here, we denote $\forall\ k = 1, \ldots, m$

$$I_1^k = \frac{1}{2\lambda}\int_{I_k} e^{-\lambda s} R^k(s)ds, \quad I_2^k = \frac{1}{2\lambda}\int_{I_k} e^{\lambda s} R^k(s)ds,$$

and also $S_+^0 = u_h(t_0^+) - u_0$ and $[u_h]_k = S_+^k + S_-^k$ with

$$S_-^k = \hat{u}_h^k - u_h(t_k^-), \quad S_+^k = u_h(t_k^+) - \hat{u}_h^k.$$

Proof. Problem (13) reads

$$\begin{aligned} \sum_{k=1}^m \int_{I_k} (-\psi' + \lambda\psi)(-\delta v' + \lambda\delta v)dt + [\psi]_k[\delta v]_k = &\sum_{k=1}^m \int_{I_k} u_h(-\delta v' + \lambda\delta v)dt - \hat{u}_h^k[\delta v]_k \\ &- \sum_{k=1}^m \int_{I_k} f\delta v dt - u_0\delta v(t_0^+), \end{aligned}$$

and selecting test functions with local support in I_k, we obtain

$$\begin{aligned} &\int_{I_k} (-\psi' + \lambda\psi)(-\delta v' + \lambda\delta v)dt - [\psi]_k\delta v(t_k^-) + [\psi]_{k-1}\delta v(t_{k-1}^+) \\ &= \int_{I_k} u_h(-\delta v' + \lambda\delta v)dt + \hat{u}_h^k\delta v(t_k^-) - \hat{u}_h^{k-1}\delta v(t_{k-1}^+) - \int_{I_k} f\delta v dt. \end{aligned} \quad (17)$$

Integrating by parts, we have that $\psi(t)$ satisfies the following m overlapping boundary value problems

$$\begin{cases} -\psi'' + \lambda^2\psi = R^k, \ \ \forall\ t \in I_k, \\ -\psi'(t_{k-1}^+) + \lambda\psi(t_{k-1}^+) + \psi(t_{k-1}^+) - \psi(t_{k-1}^-) = S_+^{k-1}, \ \ (BC_1^k) \\ \psi'(t_k^-) - \lambda\psi(t_k^-) + \psi(t_k^-) - \psi(t_k^+) = S_-^k, \ \ (BC_2^k) \end{cases} \quad (18)$$

$\forall\ k = 1, \ldots, m$. In particular, for $k = 1$ and $k = m$, we have

$$\begin{aligned} &BC_1^1 : -\psi'(t_0^+) + \lambda\psi(t_0^+) = S_+^0, \\ &BC_2^m : \psi'(t_m^-) - \lambda\psi(t_m^-) + \psi(t_m^-) = S_-^m. \end{aligned} \tag{19}$$

From the first equation of (18), we obtain

$$\psi^k(t) = C_1^k e^{\lambda t} + C_2^k e^{-\lambda t} + \frac{e^{\lambda t}}{2\lambda}\int_t^{t_k} e^{-\lambda s} R^k(s)ds - \frac{e^{-\lambda t}}{2\lambda}\int_t^{t_k} e^{\lambda s} R^k(s)ds,$$

and we now determine C_1^k and C_2^k from the boundary conditions. From BC_1^k in (18), we have $\forall\ k = 2, \ldots, m$

$$(C_1^k + I_1^k)e^{\lambda t_{k-1}} + (C_2^k - I_2^k)(1 + 2\lambda)e^{-\lambda t_{k-1}} = C_1^{k-1}e^{\lambda t_{k-1}} + C_2^{k-1}e^{-\lambda t_{k-1}} + S_+^{k-1}, \tag{20}$$

and from BC_1^1 in (19)

$$2\lambda(C_2^1 - I_2^1)e^{-\lambda t_0} = S_+^0,$$

which is the first equation in (15). Similarly, from BC_2^k in (18) we obtain $\forall\ k = 1, \ldots, m-1$

$$C_1^k e^{\lambda t_k} + C_2^k(1 - 2\lambda)e^{-\lambda t_k} - S_-^k = (C_1^{k+1} + I_1^{k+1})e^{\lambda t_k} + (C_2^{k+1} - I_2^{k+1})e^{-\lambda t_k} \tag{21}$$

and from BC_2^m in (19)

$$C_1^m e^{\lambda t_m} + C_2^m(1 - 2\lambda)e^{-\lambda t_m} = S_-^m,$$

which is the first equation in (16). From (20) and (21), we obtain the following system after adjusting the indices $\forall\ k = 1, \ldots, m-1$

$$\begin{cases} (C_1^{k+1} + I_1^{k+1})e^{\lambda t_k} + (C_2^{k+1} - I_2^{k+1})(1 + 2\lambda)e^{-\lambda t_k} = C_1^k e^{\lambda t_k} + C_2^k e^{-\lambda t_k} + S_+^k, \\ (C_1^{k+1} + I_1^{k+1})e^{\lambda t_k} + (C_2^{k+1} - I_2^{k+1})e^{-\lambda t_k} = C_1^k e^{\lambda t_k} + C_2^k(1 - 2\lambda)e^{-\lambda t_k} - S_-^k, \end{cases} \tag{22}$$

Finally, subtracting both equations in (22), we obtain the second equation in (15) and solving for C_1^k in (22), we obtain the second equation in (16). □

Corollary 1. *From Proposition 1, it holds that*

$$\begin{aligned} ||\psi||_V^2 &= \sum_{k=1}^m \int_{I_k} |-\psi' + \lambda\psi|^2 dt + [\psi]_k^2 \\ &= \sum_{k=1}^m \int_{I_k} \left| 2\lambda C_2^k e^{-\lambda t} - e^{-\lambda t}\int_t^{t_k} e^{\lambda s} R^k(s)ds \right|^2 dt + \left(-2\lambda C_2^k e^{-\lambda t_k} - S_-^k\right)^2. \end{aligned} \tag{23}$$

The error representation function ψ of Proposition 1 is given for any discrete ansatz function in $U_{h,p}$. In view of (12), we can employ the adjoint norm of the error described in Corollary 1 to perform adaptivity. However, we have not used in any place of the proof that z_h is the optimal solution. In the next proposition we give the expression for the error representation function when z_h is the solution of problem (10).

Proposition 2. *The error representation function (13) for the solution $z_h \in U_{h,p}$ of problem (10) with the variational setting defined in Section 2 is* $\forall\ k = 1, \ldots, m$

$$\psi^k(t) := \psi(t)_{|_{I_k}} = C_1^k e^{\lambda t} - \frac{S_-^k}{2\lambda} e^{\lambda(t_k - t)} + \frac{e^{\lambda t}}{2\lambda} \int_t^{t_k} e^{-\lambda s} R^k(s) ds - \frac{e^{-\lambda t}}{2\lambda} \int_t^{t_k} e^{\lambda s} R^k(s) ds, \quad (24)$$

where $R^k(t) := (u_h^k(t))' + \lambda u_h^k(t) - f(t)_{|_{I_k}}$ *is the residual at* I_k *and constants* C_1^k *are defined recursively as*

$$\begin{cases} C_1^m = -\dfrac{S_-^m}{2\lambda} e^{-\lambda t_m}, \\ C_1^k = C_1^{k+1} + I_1^{k+1} + \dfrac{e^{-\lambda t_k}}{2\lambda} [u_h]_k, \ \ \forall\ k = m-1, \ldots, 1. \end{cases} \quad (25)$$

Here, we denote $\forall\ k = 1, \ldots, m$

$$I_1^k = \frac{1}{2\lambda} \int_{I_k} e^{-\lambda s} R^k(s) ds,$$

and also $S_+^0 = u_h(t_0^+) - u_0$ *and* $[u_h]_k = S_+^k + S_-^k$ *with*

$$S_-^k = \hat{u}_h^k - u_h(t_k^-), \quad S_+^k = u_h(t_k^+) - \hat{u}_h^k.$$

Proof. From Proposition 1, we know that the error representation function $\psi(t)$ corresponding to the optimal solution z_h of problem (10) is (14). Aditionally, as z_h satisfies (10), we have that

$$(\psi, \delta v_h)_V = 0, \ \ \forall\ \delta v_h \in V_{h,p}^{opt}.$$

In particular, testing with $\hat{v}^k$ in (17) and employing (9), we obtain

$$\begin{aligned} &[\psi]_1 = 0, \\ &[\psi]_k = [\psi]_{k-1} \hat{v}^k(t_{k-1}), \ \ \forall\ k = 2, \ldots, m, \end{aligned} \quad (26)$$

which implies that $[\psi]_k = 0, \ \forall\ k = 1, \ldots, m$ and, therefore, in this case $\psi(t)$ is a globally continuous function and from (23),

$$[\psi]_k = -2\lambda C_2^k e^{-\lambda t_k} - S_-^k = 0, \ \ \forall\ k = 1, \ldots, m,$$

which lead to expressions (24) and (25). Finally, recurrence formulas (15) reduce to

$$\frac{-e^{t_k}}{2\lambda} S_-^k = I_2^k + \frac{e^{\lambda t_{k-1}}}{2\lambda} S_+^{k-1}, \ \ \forall\ k = 1, \ldots, m, \quad (27)$$

and integrating by parts in I_2^k we obtain

$$2\lambda I_2^k = e^{\lambda t_k} u_h(t_k^-) - e^{\lambda t_{k-1}} u_h(t_{k-1}^+) - \int_{I_k} f e^{\lambda t} dt, \quad (28)$$

and from the first equation in (11) we have that $\displaystyle\int_{I_k} f e^{\lambda t} dt = e^{\lambda t_k} \hat{u}_h^k - e^{\lambda t_{k-1}} \hat{u}_h^{k-1}$, therefore conditions (27) are automatically satisfied. □

Corollary 2. *From Proposition 2, it holds that*

$$\begin{aligned} ||\psi||_V^2 &= \sum_{k=1}^{m} \int_{I_k} |-\psi' + \lambda\psi|^2 dt + [\psi]_k^2 \\ &= \sum_{k=1}^{m} \int_{I_k} \left| -S_-^k e^{\lambda(t_k - t)} - e^{-\lambda t} \int_t^{t_k} e^{\lambda s} R^k(s) ds \right|^2 dt. \end{aligned} \tag{29}$$

In this particular case, the error representation function (24) can be computed backwards in time and the adjoint norm (29) is a sum of local contributions. However, both expressions are given in integral form. In the next section, we introduce an approximation to the analytical error representation function with the goal of simplifying both $\psi(t)$ in (24) and its adjoint norm (29).

4. Practical error representation

In order to obtain a computable approximation of the analytical error representation defined in Proposition 2, we consider the *practical DPG* framework [24] in this section. The idea is to select a finite dimensional subspace of V to solve both problems (7) and (13). However, we can take advantage of knowing the analytical solution of both problems. Our goal is to find a subspace of V that delivers the same optimal test functions as in (7) and a good approximation for (13).

Given the trial space $U_{h,p}$ defined in Section 2, we propose to solve both problems (7) and (13) substituting V by the following subspace

$$V_{h,r} = span\{\hat{v}^k, v_j^k, \ \forall\, j = 0, \ldots, r, \ \forall\, k = 1, \ldots, m\}, \tag{30}$$

with $r \geq p+1$ and the functions in (30) satisfying (8) and (9). We now define the discrete version of (7) as

$$\begin{cases} \text{Find } v_h \in V_{h,r} \text{ such that} \\ (v_h, \delta v_h)_V = b(z_h, \delta v_h), \ \ \forall\, \delta v_h \in V_{h,r}, \end{cases} \tag{31}$$

and the discrete version of (13) as

$$\begin{cases} \text{Find } \psi_h \in V_{h,r} \text{ such that} \\ (\psi_h, \delta v_h)_V = b(z_h, \delta v_h) - l(\delta v_h), \ \ \forall\, \delta v_h \in V_{h,r}. \end{cases} \tag{32}$$

This construction leads us to the following remarks, which are the key points of this article.

Remark 1. *The space defined in (30) is an enriched test space containing the optimal test functions corresponding to $U_{h,p}$, i.e. $V_{h,p}^{opt} \subset V_{h,r}$. It is easy to verify that the constants corresponding to v_j^k with $j = p+1, \ldots, r$ are equal to zero in system (31). Therefore, the optimal test space we obtain from (31) is exactly $V_{h,p}^{opt}$ and we can conclude that practical DPG method we propose here delivers the optimal solution (10).*

Remark 2. *We know from Propositions 1 and 2 that $\psi(t)$ includes negative exponential terms like $e^{-\lambda t}$, which is not an element of $V_{h,r}$. Therefore, problem (32) does not deliver $\psi(t) \in V$ but an approximation of it: $\psi_h(t) \in V_{h,r} \subset V$. We study this approximation in the next section by introducing a Fortin operator and a posteriori error estimates.*

Summarizing, the practical DPG method defined in this section delivers the optimal solution and an approximation of the error representation function. Finally, we give an explicit formula to compute the approximated error $\psi_h \in V_{h,r}$ for the optimal solution in (10).

Proposition 3. *The approximate error representation function (31) for the solution $z_h \in U_{h,p}$ of problem (10) with the variational setting defined in Section 2 is*

$$\psi_h(t) = \sum_{k=1}^{m} \left(\hat{\psi}_h^k \hat{v}^k + \sum_{i=0}^{r} \psi_{h,i}^k v_i^k \right), \tag{33}$$

with the coefficients satisfying the following local systems $\forall\ k = 1, \ldots, m$

$$\begin{cases} \displaystyle\sum_{i=0}^{r} \frac{h_k}{i+j+1} \psi_{h,i}^k = 0, \ \ \forall\ j = 0, \ldots, p, \\ \displaystyle\sum_{i=0}^{r} \frac{h_k}{i+j+1} \psi_{h,i}^k = \sum_{i=0}^{p} \frac{h_k}{i+j+1} u_{h,i}^k - \int_{I_k} f^k v_j^k dt - \hat{u}_h^{k-1} v_j^k(t_{k-1}), \ \ \forall\ j = p+1, \ldots, r, \end{cases} \tag{34}$$

and global continuity conditions

$$\begin{cases} \hat{\psi}_h^m = 0, \\ \hat{\psi}_h^k = \hat{\psi}_h^{k+1} \hat{v}^{k+1}(t_k) + \displaystyle\sum_{i=0}^{r} \psi_{h,i}^{k+1} v_i^{k+1}(t_k), \ \ \forall\ k = m-1, \ldots, 1. \end{cases} \tag{35}$$

Proof. From conditions (9) of the basis functions in $V_{h,r}$, we have that

$$-\psi_h' + \lambda \psi_h = \sum_{k=1}^{m} \sum_{i=0}^{r} \psi_{h,i}^k \left(\frac{t - t_{k-1}}{h_k} \right)^i, \tag{36}$$

and also

$$[\psi_h]_k = \psi_h(t_k^+) - \psi_h(t_k^-) = \hat{\psi}_h^{k+1} \hat{v}^{k+1}(t_k) + \sum_{i=0}^{r} \psi_{h,i}^{k+1} v_i^{k+1}(t_k) - \hat{\psi}_h^k. \tag{37}$$

We note that the right-hand-side of (32) vanishes for all functions in $V_{h,p}^{opt}$, i.e.,

$$(\psi_h, \delta v_h)_V = 0, \ \ \forall\ \delta v_h \in V_{h,p}^{opt} \subset V_{h,r}. \tag{38}$$

This follows directly from the fact that z_h is the solution from problem (10).

We now test problem (32) with the basis functions of $V_{h,r}$:

- If we test with $\hat{v}^k,\ \forall\ k = 2, \dots, m$, as $\hat{v}^k \in V_{h,p}^{opt}$ and it has local support in I_k, we obtain

$$\int_{I_k} (-\psi_h' + \lambda\psi_h)(-(\hat{v}^k)' + \lambda\hat{v}^k)dt - [\psi_h]_k\hat{v}^k(t_k) + [\psi_h]_{k-1}\hat{v}^k(t_{k-1}) = 0,$$

and from (9), we have

$$[\psi_h]_k = [\psi_h]_{k-1}\hat{v}^k(t_{k-1}),\ \ \forall\ k = 2, \dots, m.$$

In particular, for $\hat{v}^1$, as we do not have a jump in t_0, we obtain that $[\psi_h]_1 = 0$. Therefore, the jumps of ψ_h vanish, i.e,

$$[\psi_h]_k = 0,\ \ \forall\ k = 1, \dots, m-1,$$
$$[\psi_h]_m = -\hat{\psi}_h^m = 0,$$

which are the conditions in (35) with the jumps defined in (37). We then conclude from (35) that $\psi_h(t)$ is a globally continuous function.

- If we test with $v_j^k,\ \forall\ k = 1, \dots, m,\ \forall\ j = 0, \dots, p$, we have

$$\int_{I_k} (-\psi_h' + \lambda\psi_h)(-(\hat{v}^k)' + \lambda\hat{v}^k)dt = 0,$$

and from (36) and (9) we obtain the first equation in (34)

$$\sum_{i=0}^{r} \psi_{h,i}^k \int_{I_k} \left(\frac{t - t_{k-1}}{h_k}\right)^{i+j} dt = 0.$$

- Similarly, when we test with $v_j^k,\ \forall\ k = 1, \dots, m,\ \forall\ j = p+1, \dots, r$, we obtain the second equation in (34)

$$\sum_{i=0}^{r} \psi_{h,i}^k \int_{I_k} \left(\frac{t - t_{k-1}}{h_k}\right)^{i+j} dt = \sum_{i=0}^{p} u_{h,i}^k \int_{I_k} \left(\frac{t - t_{k-1}}{h_k}\right)^{i+j} dt - \int_{I_k} f^k v_j^k dt - \hat{u}_h^{k-1} v_j^k(t_{k-1}).$$

□

Corollary 3. *From Proposition 3, it holds that*

$$||\psi_h||_V^2 = \sum_{k=1}^{m} \int_{I_k} |-\psi_h' + \lambda\psi_h|^2 dt + [\psi_h]_k^2 = \sum_{k=1}^{m} \int_{I_k} \left| \sum_{i=0}^{r} \psi_{h,i}^k \left(\frac{t - t_{k-1}}{h_k}\right)^i \right|^2 dt. \qquad (39)$$

We observe that computing the error $\psi_h(t)$ in (33) involves another time-marching scheme that needs to be computed backwards in time. We know that $\hat{\psi}_h^m = 0$, then we can compute the local problem (34) for $k = m$ to calculate $\psi_{h,i}^m$ and then employ (35) to compute $\hat{\psi}_h^{m-1}$. We repeat this process for $k = m, \dots, 1$. However, note that the adjoint norm of $\psi_h(t)$ in (39) reduces it to solving local problems (34) and then integrate a polynomial of order r in each element, which is simpler than the expression given in Proposition 2.

Remark 3. *We can also employ (32) to approximate the error representation function of any perturbed solution $z_h \in U_{h,p}$. However, as it occurs in Proposition 1, the jumps are not zero and (32) is not a time-marching scheme but a global problem.*

5. Error analysis

In this section, we analyze the approximation of the analytical error representation given in (32) by constructing a Fortin operator [34], and introducing a posteriori error estimates similar to [3].

5.1. Fortin operator

We first recall the notion of Fortin operator [20].

Definition 1. *A linear map $\Pi : V \longrightarrow V_{h,r}$ is called a Fortin operator if it satisfies the following conditions*

$$\begin{cases} b(\delta z_h, v - \Pi v) = 0, \ \ \forall\, \delta z_h \in U_{h,p}, \\ ||\Pi v||_V \leq C_\Pi ||v||_V. \end{cases} \tag{40}$$

The constant C_Π is the operator norm and it is referred to as the Fortin constant.

In the next theorem, we construct a global Fortin operator defined in Definition 1 and we prove that it is an orthogonal projection, hence its norm is equal one.

Theorem 1. *The following operator $\Pi : V \longrightarrow V_{h,r}$ defined locally at each element I_k as*

$$\begin{cases} \displaystyle\int_{I_m} \chi_h(-\Pi v' + \lambda \Pi v)dt = \int_{I_m} \chi_h(-v' + \lambda v)dt, \ \ \forall\, \chi_h \in \mathcal{P}_r(I_m), \\ \Pi v(t_m^-) = v(t_m^-), \end{cases} \tag{41}$$

and $\forall\ k = m-1, \ldots, 1$

$$\begin{cases} \displaystyle\int_{I_k} \chi_h(-\Pi v' + \lambda \Pi v)dt = \int_{I_k} \chi_h(-v' + \lambda v)dt, \ \ \forall\, \chi_h \in \mathcal{P}_r(I_k), \\ \Pi v(t_k^-) = \Pi v(t_k^+) - [v]_k, \end{cases} \tag{42}$$

with $\mathcal{P}_r(I_k)$ denoting the space of polynomials up to order r in I_k, satisfies conditions (40). Moreover, Π is an orthogonal projection of functions from V into $V_{h,r}$ and therefore

$$|C_\Pi| \leq 1.$$

Proof. Employing the test functions defined in (30), we express $\Pi v \in V_{h,r}$ as

$$\Pi v = \sum_{k=1}^{m} \left(\hat{\alpha}^k \hat{v}^k + \sum_{i=0}^{r} \alpha_i^k v_i^k \right). \tag{43}$$

Therefore, (41) and (42) describe a square system of $m(r+2)$ unknowns and equations. We can solve (41) and (42) as a time-marching-scheme backwards in time and the value $\Pi v(t_k^+)$ is known from solving the system at I_{k+1}.

If we multiply the equations at the boundaries by real numbers $\hat{\chi}_h^k \in \mathbb{R}$ and summing up all equations in (41) and (42), we obtain

$$\sum_{k=1}^{m} \int_{I_k} \chi_h(-\Pi v' + \lambda \Pi v)dt - \hat{\chi}_h^k [\Pi v]_k = \sum_{k=1}^{m} \int_{I_k} \chi_h(-v' + \lambda v)dt - \hat{\chi}_h^k [v]_k, \ \forall \ (\chi_h, \hat{\chi}_h^1, \ldots, \hat{\chi}_h^m) \in U_{h,r},$$

or equivalently, $b(\delta\chi_h, \Pi v) = b(\delta\chi_h, v), \ \ \forall \ \delta\chi_h \in U_{h,r}$. As $U_{h,p} \subset U_{h,r}$, the first condition in Definition 1 is satisfied.

From (9) and (43), we can rewrite (41) and (42) as

$$\begin{cases} \displaystyle\sum_{i=0}^{r} \alpha_i^m \int_{I_m} \left(\frac{t - t_{m-1}}{h_m}\right)^{i+j} dt = \int_{I_m} \left(\frac{t - t_{m-1}}{h_m}\right)^{j} (-v' + \lambda v)dt, \ \ \forall \ j = 0, \ldots, r, \\ \hat{\alpha}^m = v(t_m^-), \end{cases} \tag{44}$$

and $\forall \ k = m-1, \ldots, 1$

$$\begin{cases} \displaystyle\sum_{i=0}^{r} \alpha_i^k \int_{I_k} \left(\frac{t - t_{k-1}}{h_k}\right)^{i+j} dt = \int_{I_k} \left(\frac{t - t_{k-1}}{h_k}\right)^{j} (-v' + \lambda v)dt, \ \ \forall \ j = 0, \ldots, r, \\ \hat{\alpha}^k = \hat{\alpha}^{k+1}\hat{v}^{k+1}(t_k^+) + \displaystyle\sum_{i=0}^{r} \alpha^{k+1} v_i^{k+1}(t_k^+) - [v]_k. \end{cases} \tag{45}$$

To see that Π is a projection, we select in the right-and-side of (44) and (45), $v = \Pi w \in V_{h,r}$ with $w \in V$ and we express

$$\Pi w = \sum_{k=1}^{m} \left(\hat{\beta}^k \hat{v}^k + \sum_{i=0}^{r} \beta_i^k v_i^k \right).$$

From (44) and the first equation in (45), it is easy to see that $\beta_i^k = \alpha_i^k, \ \forall \ k = 1, \ldots, m, \ \forall \ i = 0, \ldots, r$, and $\hat{\beta}^m = \hat{\alpha}^m$. From the second equation in (45), we have

$$\hat{\beta}^k = \hat{\beta}^{k+1}\hat{v}^{k+1}(t_k^+) + \sum_{i=0}^{r} \beta_i^{k+1} v_i^{k+1}(t_k^+) + \hat{\alpha}^k - \hat{\alpha}^{k+1} v(t_k^+) - \sum_{i=0}^{r} \alpha_i^{k+1} v_i^{k+1}(t_k^+),$$

which reduces to $\hat{\beta}^k - \hat{\beta}^{k+1}\hat{v}^{k+1}(t_k^+) = \hat{\alpha}^k - \hat{\alpha}^{k+1} v^{k+1}(t_k^+), \ \forall \ k = m-1, \ldots, 1$. As $\hat{\beta}^m = \hat{\alpha}^m$, we have that $\hat{\beta}^k = \hat{\alpha}^k, \ \forall \ k = m-1, \ldots, 1$. Therefore, $\Pi(\Pi w) = \Pi w, \ \forall \ w \in V$ so Π is a projection.

Finally, to prove that Π is an orthogonal projection, we need to see that $(v - \Pi v, \Pi v)_V = 0, \ \forall \ v \in V$. Considering the inner product defined in (6), we have from (9) that the optimal

test functions satisfy $\forall\ k = 2, \ldots, m$

$$(\hat{v}^k, \delta v)_V = -[\delta v]_k + \hat{v}^k(t_{k-1}^+)[\delta v]_{k-1} = b((0,0,\ldots,\underbrace{1}_{k},\ldots,0), \delta v) + \hat{v}^k(t_{k-1}^+)[\delta v]_{k-1},$$

$$\begin{aligned}(v_i^k, \delta v)_V &= \int_{I_k} \left(\frac{t - t_{k-1}}{h_k}\right)^i (-\delta v + \lambda \delta v)dt + v_i^k(t_{k-1}^+)[\delta v]_{k-1} \\ &= b\left(\left(\left(\frac{t - t_{k-1}}{h_k}\right)^i, 0, \ldots, 0\right), \delta v\right) + v_i^k(t_{k-1}^+)[\delta v]_{k-1},\ \forall\ i = 0, \ldots, r,\end{aligned}$$

and for $k = 1$ we obtain the same expression but without the jump term. Therefore, from these equalities and the definition of Π we obtain

$$\begin{aligned}(\Pi v, \Pi v)_V &= \sum_{k=1}^{m} \hat{\alpha}^k(\hat{v}^k, \Pi v)_V + \sum_{k=1}^{m}\sum_{i=0}^{r} \alpha_i^k(v_i^k, \Pi v)_V \\ &= \sum_{k=1}^{m} \hat{\alpha}^k b((0,0,\ldots,\underbrace{1}_{k},\ldots,0), \Pi v) + \sum_{k=2}^{m} \hat{v}^k(t_{k-1}^+)[\Pi v]_{k-1} \\ &+ \sum_{k=1}^{m}\sum_{i=0}^{r} \alpha_i^k b\left(\left(\left(\frac{t - t_{k-1}}{h_k}\right)^i, 0, \ldots, 0\right), \Pi v\right) + \sum_{k=2}^{m}\sum_{i=0}^{r} v_i^k(t_{k-1}^+)[\Pi v]_{k-1} \\ &= \sum_{k=1}^{m} \hat{\alpha}^k b((0,0,\ldots,\underbrace{1}_{k},\ldots,0), v) + \sum_{k=2}^{m} \hat{v}^k(t_{k-1}^+)[v]_{k-1} \\ &+ \sum_{k=1}^{m}\sum_{i=0}^{r} \alpha_i^k b\left(\left(\left(\frac{t - t_{k-1}}{h_k}\right)^i, 0, \ldots, 0\right), v\right) + \sum_{k=2}^{m}\sum_{i=0}^{r} v_i^k(t_{k-1}^+)[v]_{k-1} \\ &= \sum_{k=1}^{m} \hat{\alpha}^k(\hat{v}^k, v)_V + \sum_{k=1}^{m}\sum_{i=0}^{r} \alpha_i^k(v_i^k, v)_V = (\Pi v, v)_V.\end{aligned}$$

□

5.2. A posteriori error estimation

We first analyze the continuity and the inf-sup constants of the continuous broken formulation (4) in the next theorem.

Theorem 2. *The bilinear form defined in (5) satisfies the following inf-sup and continuity conditions*

$$\gamma||z||_U \leq \sup_{0 \neq v \in V} \frac{|b(z,v)|}{||v||_V} \leq M||z||_U, \tag{46}$$

with $\gamma = M = 1$ *and the following uniqueness condition holds*

$$\{v \in V \mid b(z,v) = 0,\ \forall\ z \in U\ \} = \{0\}. \tag{47}$$

Proof. We first proof the uniqueness condition (47). We have that

$$b(z,v) = \sum_{k=1}^{m} \int_{I_k} u(-v' + \lambda v)dt - \hat{u}^k[v]_k = 0, \ \ \forall\, z \in U.$$

In particular, it holds for $z = (0, 1, \ldots, 1)$, therefore $[v]_k = 0,\ \forall\, k = 1, \ldots, m$. This means that $v \in H^1(\Omega)$ and $v(t_m) = 0$. Now, selecting functions u with local support in I_k, we obtain that $v(t)$ satisfies

$$\begin{cases} -v' + \lambda v = 0,\ \forall\, t \in I_k, \\ \qquad [v]_k = 0,\ \forall\, k = 1, \ldots, m-1, \\ \quad v(t_m) = 0, \end{cases} \tag{48}$$

The first equation in (48) leads to $v(t)_{|_{I_k}} = \alpha_k e^{\lambda(t-t_k)},\ \forall\, k = 1, \ldots, m$, and from the second equation in (48), we have

$$\alpha_{k+1} e^{\lambda h_k} = \alpha_k, \ \ \forall\, k = 1, \ldots, m-1.$$

The last condition in (48) implies that $\alpha_m = 0$ and therefore $\alpha_k = 0,\ \forall\, k = 1, \ldots, m$ and (47) holds. The continuity constant of the bilinear form holds directly from the Cauchy-Schwarz inequality

$$\begin{aligned} \sup_{0 \neq v \in V} \frac{|b(z,v)|^2}{||v||_V^2} &= \sup_{0 \neq v \in V} \frac{\left| \sum_{k=1}^{m} \int_{I_k} u(-v' + \lambda v)dt - \hat{u}^k[v]_k \right|^2}{||v||_V^2} \\ &\leq \sup_{0 \neq v \in V} \frac{\left(\sum_{k=1}^{m} \int_{I_k} |u|^2 dt + |\hat{u}^k|^2 \right) \left(\sum_{k=1}^{m} \int_{I_k} |-v' + \lambda v|^2 dt + [v]_k^2 \right)}{||v||_V^2} \leq ||z||_U^2. \end{aligned} \tag{49}$$

For the inf-sup condition, we test with $v = u' + \lambda u$ in I_k and $[v]_k = \hat{u}^k$ and we obtain

$$\sup_{0 \neq v \in V} \frac{|b(z,v)|^2}{||v||_V^2} \geq \frac{\left| \sum_{k=1}^{m} \int_{I_k} |u|^2 dt + |\hat{u}^k|^2 \right|^2}{\sum_{k=1}^{m} \int_{I_k} |u|^2 dt + |\hat{u}^k|^2} = ||z||_U^2.$$

□

In general, Theorem 2 implies that the analytical error representation function $\psi(t)$ provides a reliable and efficient error control of the error of the solution in the norm of U.

In other words, $||\psi||_V$ is both an upper bound and a lower bound of $||z - z_h||_U$. It follows directly form (12) and (46)

$$\frac{1}{M}||\psi||_V \leq ||z - z_h||_U \leq \frac{1}{\gamma}||\psi||_V.$$

In this case, as $M = \gamma = 1$, the equality $||\psi||_V = ||z - z_h||_U$ holds.

The next theorem proves, following the arguments in [3], that the approximated error representation function $\psi_h(t)$ introduced in (32) is reliable and efficient. For that, we need the Fortin operator defined in Section 5.1.

Theorem 3. *The approximated error representation function (32) provides a reliable and efficient error control of the analytical error representation function (13), i.e.,*

$$C_1||\psi_h||_V \leq ||\psi||_V \leq C_2||\psi_h||_V + osc, \tag{50}$$

with constants $C_1 = 1$ *and* $C_2 = \sqrt{1 + C_\Pi^2}$. *Here,* $osc = ||l \circ (I - \Pi)||_{V'}$ *is the oscillation term where* V' *is the dual space of* V *and* $l \in V'$ *is the linear form defined in (5).*

Proof. We first denote $\varepsilon = \psi - \psi_h \in V$. Restricting (13) to $V_{h,r}$ and subtracting (32), we obtain

$$(\varepsilon, \delta v_h)_V = 0, \ \ \forall\, v_h \in V_{h,r}, \tag{51}$$

and in particular $(\varepsilon, \psi_h)_V = 0$. Therefore, from the Pythagorean theorem, we obtain

$$||\psi||_V^2 = ||\varepsilon||_V^2 + ||\psi_h||_V^2. \tag{52}$$

which implies the first inequality in (50). Now, we bound $||\varepsilon||_V^2$ and for that we employ that $\Pi\varepsilon \in V_{h,r}$, so from (51) and (40), we have

$$\begin{aligned} (\varepsilon, \Pi\varepsilon)_V &= 0, \\ b(z_h, \varepsilon - \Pi\varepsilon) &= 0, \ \forall\, z_h \in U_h. \end{aligned} \tag{53}$$

Therefore, employing (53) and the definition of (13), we obtain

$$\begin{aligned} ||\varepsilon||_V^2 &= (\varepsilon, \varepsilon)_V = (\varepsilon, \varepsilon - \Pi\varepsilon)_V = (\psi, \varepsilon - \Pi\varepsilon)_V - (\psi_h, \varepsilon - \Pi\varepsilon)_V \\ &= (\psi, \varepsilon - \Pi\varepsilon)_V + (\psi_h, \Pi\varepsilon)_V = l(\varepsilon - \Pi\varepsilon) - b(z_h, \varepsilon - \Pi\varepsilon) + (\psi_h, \Pi\varepsilon)_V \\ &= l(\varepsilon - \Pi\varepsilon) + (\psi_h, \Pi\varepsilon)_V. \end{aligned} \tag{54}$$

Finally, from (40) we get

$$||\varepsilon||_V^2 \leq ||l \circ (I - \Pi)||_{V'}||\varepsilon||_V + ||\psi_h||_V C_\Pi||\varepsilon||_V,$$

and from (52)

$$||\psi||_V^2 \leq ||\psi_h||_V^2 + (osc + C_\Pi||\psi_h||_V)^2 \leq \left(\sqrt{1 + C_\Pi^2}||\psi_h||_V + osc\right)^2,$$

which leads to the second inequality in (50). □

Remark 4. *For a sharper upper bound in (50) with $C_2 = C_\Pi$, we refer to [31]. In Theorem 3, the oscillation term osc measures the data approximation error. In this article, the oscillation term will be of higher order.*

The introduction of the Fortin operator in this section is consistent with the fact that our practical DPG method delivers the optimal solution. We know from [10] that the optimal DPG method inherits the stability from the continuous problems, i.e. $\gamma_h \geq \gamma$, where γ_h is the discrete inf-sup constant. We also know that $\gamma_h \geq \frac{\gamma}{C_\Pi}$ holds for the practical DPG method in general where the optimal test functions are approximated. In our case, as we have proved that $|C_\Pi| \leq 1$, we have that

$$\gamma_h \geq \frac{\gamma}{C_\Pi} \geq \gamma.$$

Therefore, in this article we present a practical DPG method that delivers the optimal solution and an approximate error representation function ψ_h that satisfies

$$||\psi_h||_V \leq ||\psi||_V \leq \sqrt{2}||\psi_h||_V + osc.$$

In the numerical results in the next section, we employ the element contributions of $||\psi_h||_V$ as error indicators to guide the adaptivity in time. For that, we employ the classical Dörfler marking strategy [17] with parameter $\theta \in [0, 1]$. Note that, as we have a time-marching scheme, we only need to re-compute the values of the solution in the elements to the right of the first marked element in each iteration.

6. Numerical results

In this section, we present numerical results of adaptivity in time for both parabolic and hyperbolic problems. For the space discretization, we employ a Bubnov-Galerkin method with piecewise linear functions. We employ the *EXPINT* [2] package in MATLAB for the evaluation of the $\varphi-$functions.

6.1. Approximation of the Riesz representation

Here, we show an example of how close is the solution of (32) to (13) for a given right-hand-side. First, we consider a single element and we define the following functional

$$\mathcal{R}(v) = \int_0^1 f(t)v(t)dt,$$

with $f(t) = t^p$ and $p \geq 0$. and we solve the following Riesz representation problem

$$\begin{cases} \text{Find } \psi \in V \text{ such that} \\ (\psi, \delta v)_V = \mathcal{R}(\delta v), \ \ \forall\, \delta v \in V, \end{cases} \tag{55}$$

and also its discrete version

$$\begin{cases} \text{Find } \psi_h \in V_{h,r} \text{ such that} \\ (\psi_h, \delta v_h)_V = \mathcal{R}(\delta v_h), \quad \forall\, \delta v_h \in V_{h,r}. \end{cases} \tag{56}$$

We know the analytical solution ψ from Proposition 1 and we study its approximation ψ_h for different values of r, p and λ.

Figure 2 shows the solution of (55) and (56) for $\lambda = 1$ and different values of p and r. Figure 3 presents the solutions for $p = 0$, $r = 1$ and different values of λ. From both figures, we select $r = p + 1$ to approximate the analytical function ψ.

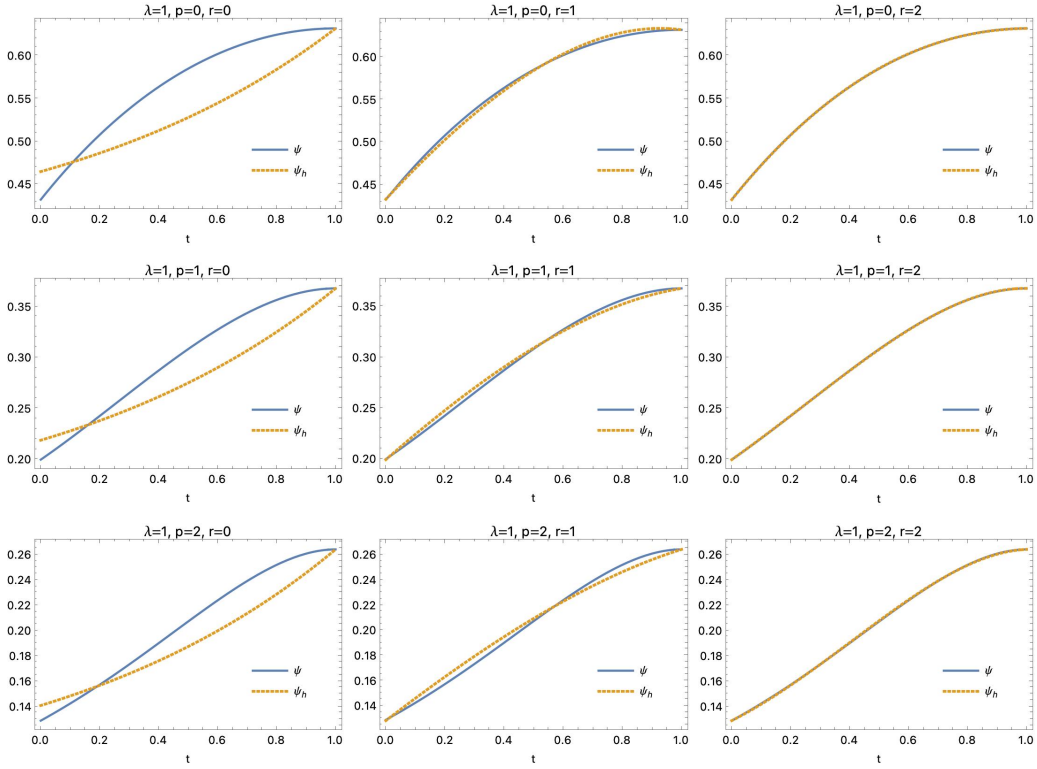

Figure 2: Functions ψ and ψ_h for $\lambda = 1$ and different values of p and r.

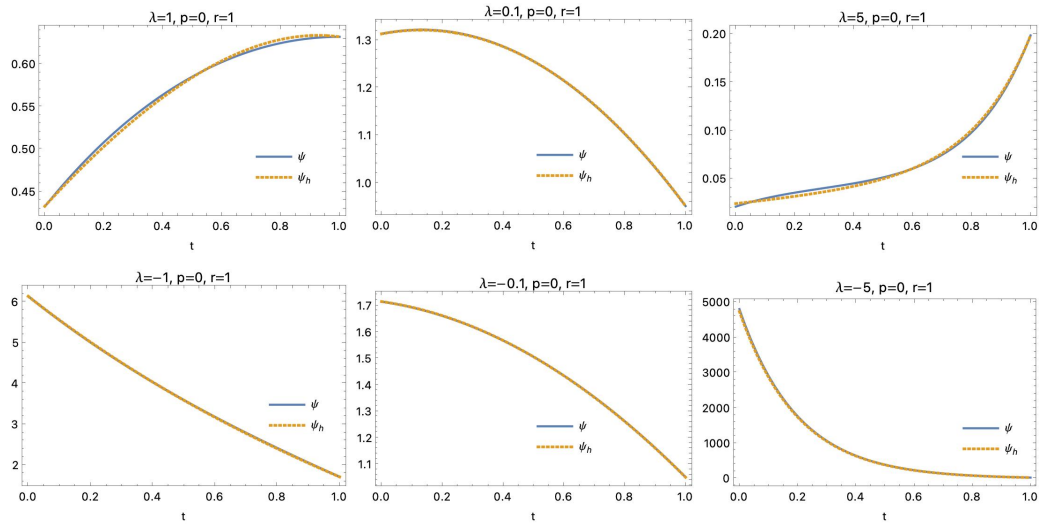

Figure 3: Functions ψ and ψ_h for $p = 0$, $r = 1$ and different values of λ.

6.2. Parabolic problem: single ODE

We consider a similar example as in [33]. In (1), we set $f(t) = \dfrac{M}{e^M - 1}$, $M = 30$, $\lambda = -M$ and $I = (0, 1]$. The exact solution to this problem is

$$u(t) = \frac{e^{M(t-1)} - e^{-M}}{1 - e^{-M}}.$$

Figure 4 shows the convergence of the exact error for $p = 0, 1, 2$ for uniform refinements and for adaptive refinements employing the Dörfler strategy with $\theta = 0.5$ and enriched test space with $r = p + 1$. We conclude that to achieve a desirable error, the adaptive strategy needs about an order of magnitude less degrees of freedom than when employing uniform refinements. Figure 5 presents the adapted solutions for $p = 0, 1, 2$ after a fixed number of iterations and the corresponding local error discrete representation functions $-(\psi_h^k(t))' + \lambda\psi_h^k(t)$. Note that from (9), these functions are polynomials of order r at each element. Finally, Figure 6 shows the convergence of the exact error for $p = 0, 1, 2$ with uniform refinements and the convergence of the discrete error $||\psi_h||_V$ for $r = p + 1$. We conclude that $||\psi_h||_V$ is an efficient and reliable error control to perform adaptivity.

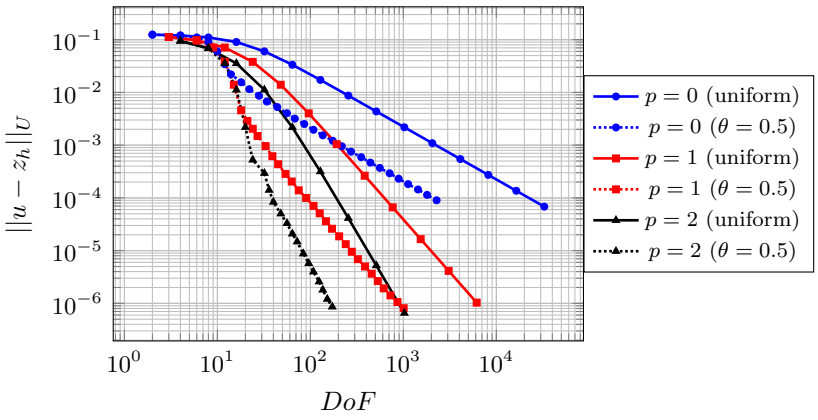

Figure 4: Convergence of the exact error for $p = 0$, $p = 1$ and $p = 2$ performing uniform refinements and the Dörfler adaptive strategy with $\theta = 0.5$.

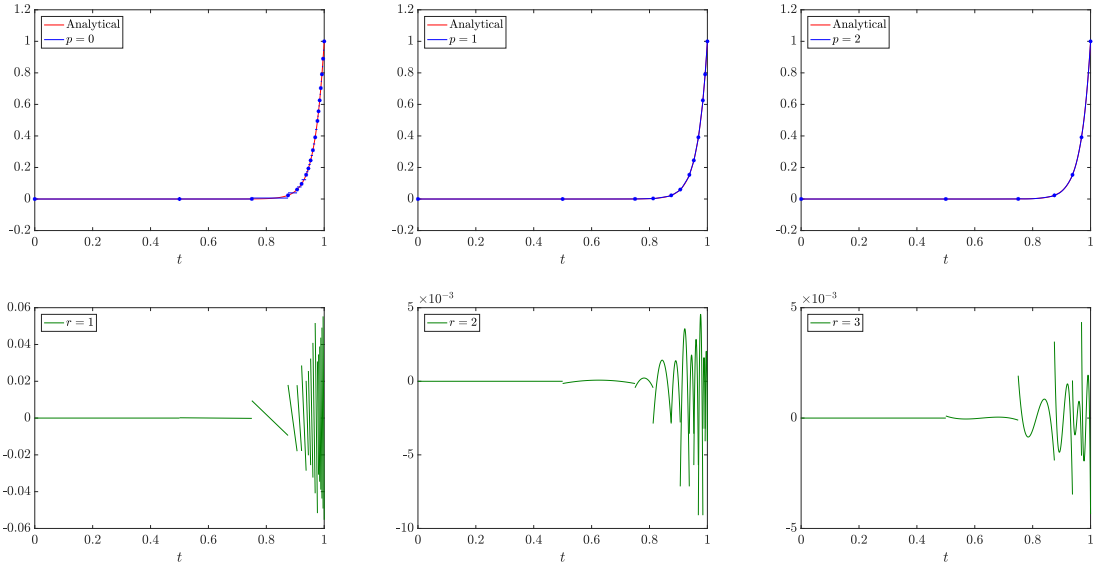

Figure 5: Adapted solution with $p = 0$, $p = 1$ and $p = 2$ for a fixed number of iterations (top row) and the corresponding local error contributions for $r = p + 1$ (bottom row).

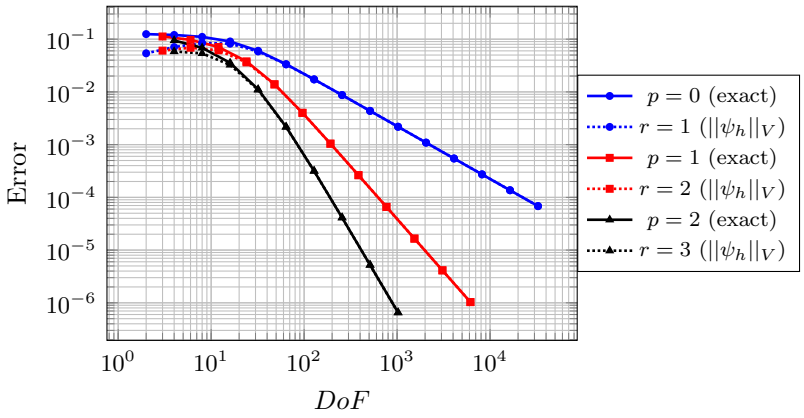

Figure 6: Convergence of the exact error for $p = 0$, $p = 1$ and $p = 2$ and the error estimator $||\psi_h||_V$ for $r = p + 1$ when performing uniform refinements.

6.3. Parabolic problem: 1D+time

We consider the following 1D+time parabolic problem that we introduced in [33]

$$\begin{cases} \dfrac{\partial u}{\partial t} - \alpha^2 \dfrac{\partial^2 u}{\partial x^2} = f(x,t), & \forall\ (x,t) \in \Omega \times I, \\ u(x,t) = 0, & \forall\ (x,t) \in \partial\Omega \times I, \\ u(x,0) = u_0(x), & \forall\ x \in \Omega. \end{cases} \tag{57}$$

We set $\Omega = (0,1)$, $I = (0, 0.5]$ and the data of the problem corresponding to the exact solution

$$u(x,t) = e^{-2\pi^2 t} sin(\pi x).$$

Figure 7 shows the adapted solutions and cross sections at $x = 0.5$ for $p = 0, 1, 2$ and 600 elements in space and $\theta = 0.5$. Figure 8 presents the corresponding error representation functions and their cross sections at $x = 0.5$. In this case, the errors are space-time tensor products with polynomials of order $r = p + 1$ in time. Figure 9 compares the relative error of the solutions when we perform uniform refinements and adaptivity with 600 elements in space and $\theta = 0.5$. We conclude that the adaptive strategy is more efficient. Finally, Figure 10 shows the convergence of the relative errors when we employ 50 elements in space. We observe that the adaptive strategy in time stops converging when the error in space becomes dominant, as expected.

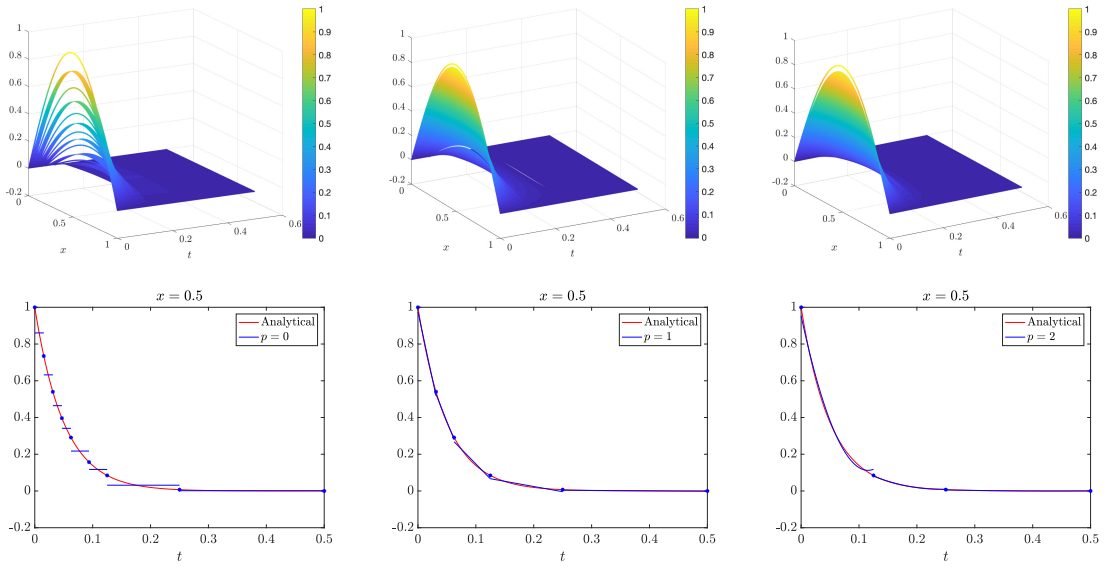

Figure 7: Adapted solution with $p = 0$, $p = 1$ and $p = 2$ for a fixed number of iterations (top row) and the corresponding cross sections at $x = 0.5$ (bottom row).

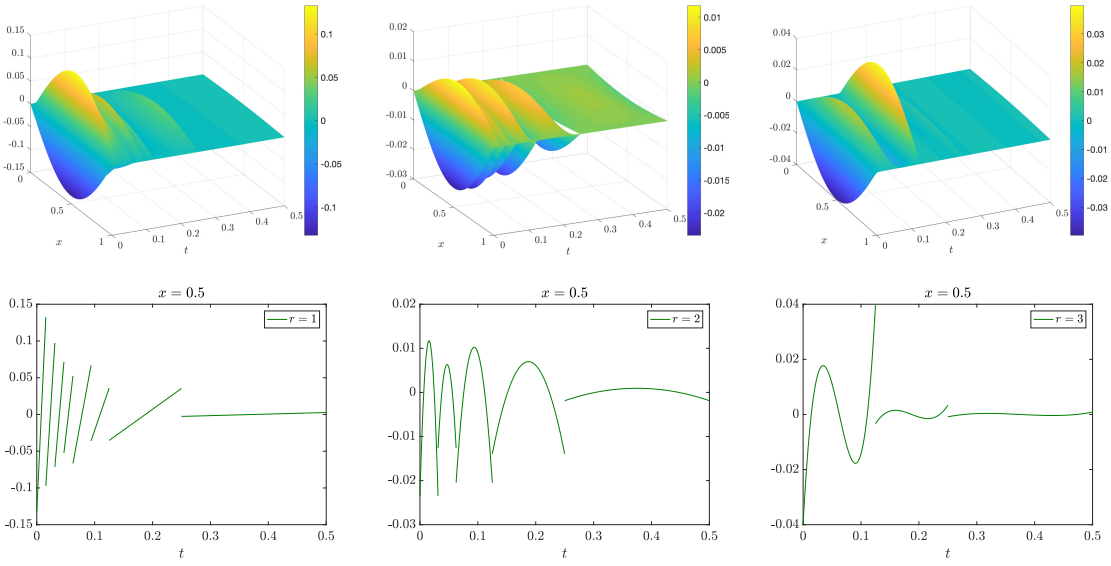

Figure 8: Error representation functions with $p = 0$, $p = 1$ and $p = 2$ for a fixed number of iterations (top row) and the corresponding cross sections at $x = 0.5$ (bottom row).

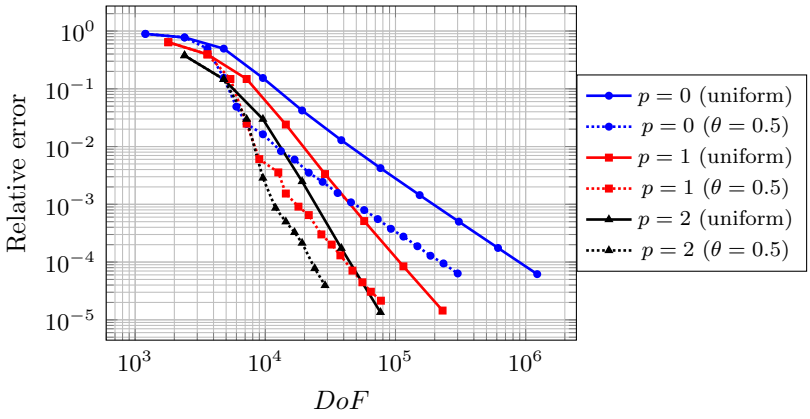

Figure 9: Relative error for $p = 0$, $p = 1$ and $p = 2$ when performing uniform refinements and the Dörfler adaptive strategy with $\theta = 0.5$. Numer of elements in space: 600.

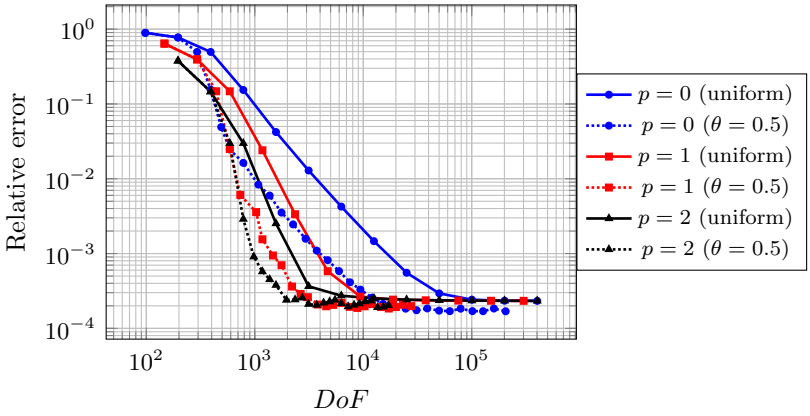

Figure 10: Relative error for $p = 0$, $p = 1$ and $p = 2$ when performing uniform refinements and the Dörfler adaptive strategy with $\theta = 0.5$. Number of elements in space: 50.

6.4. Hyperbolic problem

We consider the model hyperbolic problem presented in [32]

$$\begin{cases} U'(t) + AU(t) = F(t), & \text{in } I, \\ U(0) = U_0, \end{cases}$$

where $v = u'$ and

$$U(t) = \begin{bmatrix} u(t) \\ v(t) \end{bmatrix}, \; A = \begin{bmatrix} 0 & -1 \\ \alpha^2 & 0 \end{bmatrix}, \; F(t) = \begin{bmatrix} 0 \\ f(t) \end{bmatrix}, \; U_0 = \begin{bmatrix} u_0 \\ v_0 \end{bmatrix}.$$

In this example, we set the data corresponding to the following exact solution

$$U(t) = \begin{bmatrix} e^{\beta t}\sin(\gamma t) \\ \beta e^{\beta t}\sin(\gamma t) + \gamma e^{\beta t}\cos(\gamma t) \end{bmatrix}$$

in $I = (0, 1]$ with $\beta = -2\pi$ and $\gamma = 18\pi$.

Figure 11 displays the convergence of the exact error for $p = 0, 1, 2$ for uniform refinements and for adaptive refinements fixing $\theta = 0.5$ and $r = p + 1$. Figures 12 and 13 present the adapted solutions for $p = 0, 1, 2$ and the corresponding local error functions for $u(t)$ and $v(t)$, respectively. In this case, as explained in [33], the source is time dependent and $p = 0$ is insufficient to obtain a good approximation since we would require a very fine mesh. We observe here that for $p = 2$, the error of integrating the source is of lowest order and we obtain a good adapted solution after a few iterations.

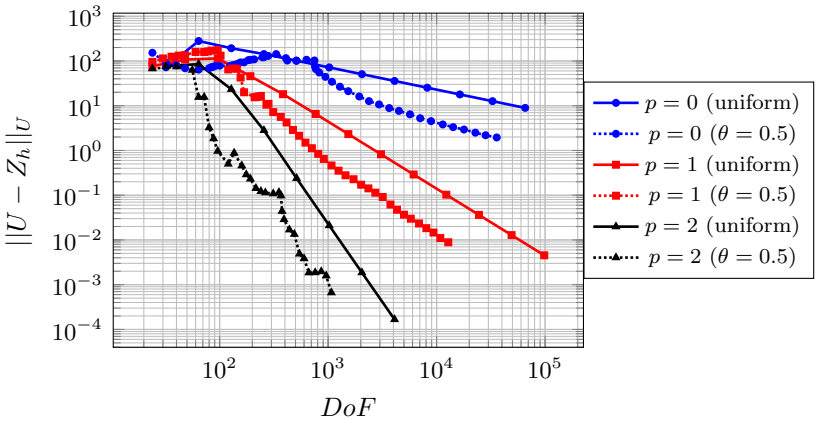

Figure 11: Convergence of the exact error for $p = 0$, $p = 1$ and $p = 2$ performing uniform refinements and the Dörfler adaptive strategy with $\theta = 0.5$.

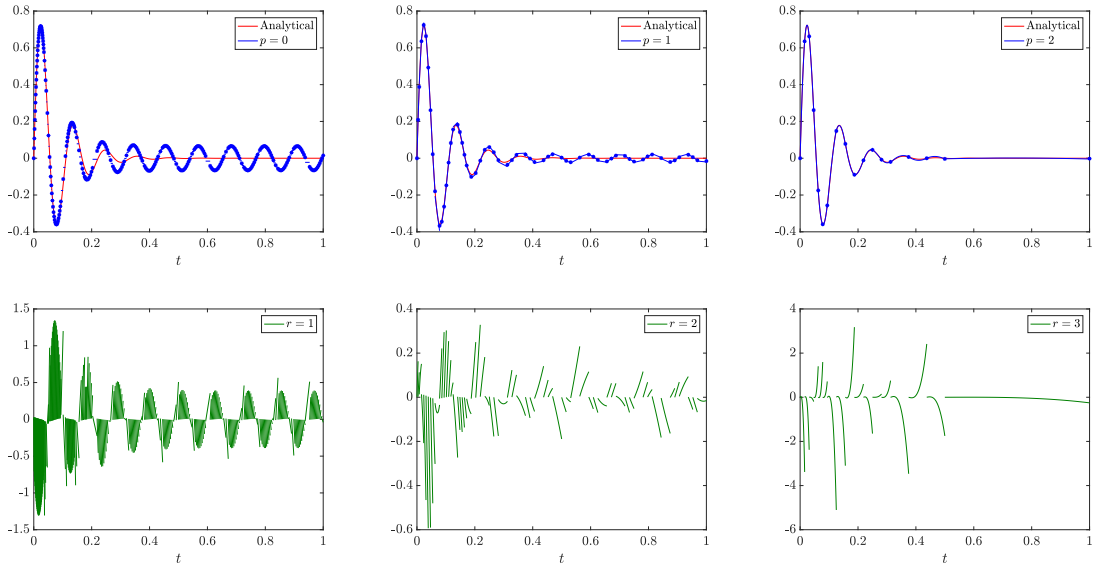

Figure 12: Adapted solution of $u(t)$ with $p = 0$, $p = 1$, and $p = 2$ for a fixed number of iterations (top row) and the corresponding local error contributions for $r = p + 1$ (bottom row).

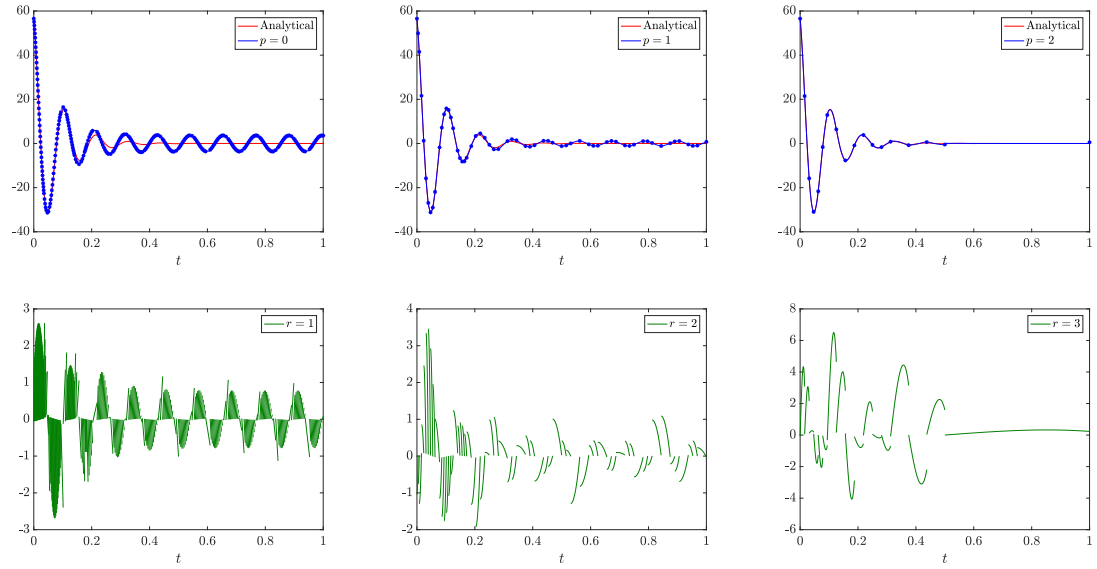

Figure 13: Adapted solution of $v(t)$ with $p = 0$, $p = 1$, and $p = 2$ for a fixed number of iterations (top row) and the corresponding local error contributions for $r = p + 1$ (bottom row).

7. Conclusions and future work

In this article, we study an error representation function to perform adaptivity in time in the DPG time-marching scheme we recently introduced in [32, 33]. We apply the DPG method in the time variable only so we can compute analytically the error representation function by inverting the Riesz operator of the residual. However, in order to obtain computable error estimators, we approximate the analytical error by enriching the test space. The enriched test space we propose contains the analytical optimal test functions so our method still delivers the optimal DPG solution. We compute both the solution and the error contributions in a time marching-scheme that has a few more equations than the ones presented in [32, 33]. We prove via analysis confirmed with numerical evidence that our proposed approximation error is reliable and efficient to perform adaptivity.

Possible extensions of this work include: (a) to combine the adaptivity in time together with adaptivity in space for the Bubnov-Galerkin method; (b) to combine the adaptive DPG-based time-marching scheme together with DPG in space; (c) to design goal-oriented adaptive strategies; (d) to extend the method to non-linear problems.

Acknowledgements

Judit Muñoz-Matute and David Pardo have received funding from the European Union's Horizon 2020 research and innovation programme under the Marie Sklodowska-Curie grant agreement No 777778 (MATHROCKS), the Project of the Spanish Ministry of Science and Innovation with reference PID2019-108111RB-I00 (FEDER/AEI), the BCAM "Severo Ochoa" accreditation of excellence (SEV-2017-0718), and the Basque Government through the BERC 2018-2021 program, and the Consolidated Research Group MATHMODE (IT1294-19) given by the Department of Education.

Judit Muñoz-Matute has also received founding from the Basque Government through the postdoctoral program for the improvement of doctor research staff (POS_2019_1_0001).

David Pardo has also received funding from the European POCTEFA 2014-2020 Project PIXIL (EFA362/19) by the European Regional Development Fund (ERDF) through the Interreg V-A Spain-France-Andorra programme, the two Elkartek projects 3KIA (KK-2020/00049) and MATHEO (KK-2019-00085) and, the Project "Artificial Intelligence in BCAM number EXP. 2019/00432".

Leszek Demkowicz was partially supported with NSF grant No. 1819101.

References

[1] A. V. Astaneh, F. Fuentes, J. Mora, and L. Demkowicz. High-order polygonal discontinuous Petrov–Galerkin (PolyDPG) methods using ultraweak formulations. *Computer Methods in Applied Mechanics and Engineering*, 332:686–711, 2018.

[2] H. Berland, B. Skaflestad, and W. M. Wright. EXPINT—A MATLAB package for exponential integrators. *ACM Transactions on Mathematical Software (TOMS)*, 33(1):4–es, 2007.

[3] C. Carstensen, L. Demkowicz, and J. Gopalakrishnan. A posteriori error control for DPG methods. *SIAM Journal on Numerical Analysis*, 52(3):1335–1353, 2014.

[4] C. Carstensen, L. Demkowicz, and J. Gopalakrishnan. Breaking spaces and forms for the DPG method and applications including Maxwell equations. *Computers & Mathematics with Applications*, 72(3):494–522, 2016.

[5] J. Chan, N. Heuer, T. Bui-Thanh, and L. Demkowicz. A robust DPG method for convection-dominated diffusion problems II: Adjoint boundary conditions and mesh-dependent test norms. *Computers & Mathematics with Applications*, 67(4):771–795, 2014.

[6] L. Demkowicz, T. Führer, N. Heuer, and X. Tian. The double adaptivity paradigm: (How to circumvent the discrete inf–sup conditions of Babuška and Brezzi). *Computers & Mathematics with Applications*, 95:41–66, 2021.

[7] L. Demkowicz and J. Gopalakrishnan. A class of discontinuous Petrov–Galerkin methods. Part I: The transport equation. *Computer Methods in Applied Mechanics and Engineering*, 199(23-24):1558–1572, 2010.

[8] L. Demkowicz and J. Gopalakrishnan. Analysis of the DPG method for the Poisson equation. *SIAM Journal on Numerical Analysis*, 49(5):1788–1809, 2011.

[9] L. Demkowicz and J. Gopalakrishnan. A class of discontinuous Petrov–Galerkin methods. Part II: Optimal test functions. *Numerical Methods for Partial Differential Equations*, 27(1):70–105, 2011.

[10] L. Demkowicz and J. Gopalakrishnan. An overview of the discontinuous Petrov–Galerkin method. In *Recent developments in discontinuous Galerkin finite element methods for partial differential equations*, pages 149–180. Springer, 2014.

[11] L. Demkowicz and J. Gopalakrishnan. Discontinuous Petrov–Galerkin (DPG) method. *Encyclopedia of Computational Mechanics Second Edition*, pages 1–15, 2017.

[12] L. Demkowicz, J. Gopalakrishnan, and B. Keith. The DPG-star method. *Computers & Mathematics with Applications*, 79(11):3092–3116, 2020.

[13] L. Demkowicz, J. Gopalakrishnan, I. Muga, and J. Zitelli. Wavenumber explicit analysis of a DPG method for the multidimensional Helmholtz equation. *Computer Methods in Applied Mechanics and Engineering*, 213:126–138, 2012.

[14] L. Demkowicz, J. Gopalakrishnan, S. Nagaraj, and P. Sepúlveda. A spacetime DPG method for the Schrödinger equation. *SIAM Journal on Numerical Analysis*, 55(4):1740–1759, 2017.

[15] L. Demkowicz, J. Gopalakrishnan, and A. H. Niemi. A class of discontinuous Petrov–Galerkin methods. Part III: Adaptivity. *Applied numerical mathematics*, 62(4):396–427, 2012.

[16] L. Demkowicz and N. Heuer. Robust DPG method for convection-dominated diffusion problems. *SIAM Journal on Numerical Analysis*, 51(5):2514–2537, 2013.

[17] W. Dörfler. A convergent adaptive algorithm for Poisson's equation. *SIAM Journal on Numerical Analysis*, 33(3):1106–1124, 1996.

[18] T. Ellis, J. Chan, and L. Demkowicz. Robust DPG methods for transient convection-diffusion. In *Building bridges: connections and challenges in modern approaches to numerical partial differential equations*, pages 179–203. Springer, 2016.

[19] T. Ellis, L. Demkowicz, J. Chan, and R. Moser. Space-time DPG: Designing a method for massively parallel CFD. ICES report. *The Institute for Computational Engineering and Sciences, The University of Texas at Austin*, pages 14–32, 2014.

[20] M. Fortin. An analysis of the convergence of mixed finite element methods. *RAIRO. Analyse numérique*, 11(4):341–354, 1977.

[21] T. Führer, N. Heuer, and J. S. Gupta. A time-stepping DPG scheme for the heat equation. *Computational Methods in Applied Mathematics*, 17(2):237–252, 2017.

[22] T. Führer, N. Heuer, and M. Karkulik. Analysis of backward Euler primal DPG methods. *arXiv preprint arXiv:2103.12181*, 2021.

[23] T. Führer and M. Karkulik. Space–time least-squares finite elements for parabolic equations. *Computers & Mathematics with Applications*, 92:27–36, 2021.

[24] J. Gopalakrishnan and W. Qiu. An analysis of the practical DPG method. *Mathematics of Computation*, 83(286):537–552, 2014.

[25] J. Gopalakrishnan and P. Sepúlveda. A space-time DPG method for the wave equation in multiple dimensions. *Space-Time Methods. Applications to Partial Differential Equations*, pages 129–154, 2017.

[26] S. Henneking and L. Demkowicz. A numerical study of the pollution error and DPG adaptivity for long waveguide simulations. *Computers & Mathematics with Applications*, 95:85–100, 2021.

[27] N. J. Higham and E. Hopkins. A catalogue of software for matrix functions. version 3.0. 2020.

[28] M. Hochbruck and A. Ostermann. Exponential integrators. *Acta Numerica*, 19:209–286, 2010.

[29] M. Hochbruck and A. Ostermann. Exponential multistep methods of Adams-type. *BIT Numerical Mathematics*, 51(4):889–908, 2011.

[30] M. Hochbruck, A. Ostermann, and J. Schweitzer. Exponential Rosenbrock-type methods. *SIAM Journal on Numerical Analysis*, 47(1):786–803, 2009.

[31] B. Keith. *New ideas in adjoint methods for PDEs: A saddle-point paradigm for finite element analysis and its role in the DPG methodology.* PhD thesis, Oden Institute for Computational Engineering and Sciences, The University of Texas at Austin, 2018.

[32] J. Muñoz-Matute, D. Pardo, and L. Demkowicz. A DPG-based time-marching scheme for linear hyperbolic problems. *Computer Methods in Applied Mechanics and Engineering*, 373:113539, 2021.

[33] J. Muñoz-Matute, D. Pardo, and L. Demkowicz. Equivalence between the DPG method and the exponential integrators for linear parabolic problems. *Journal of Computational Physics*, 429:110016, 2021.

[34] S. Nagaraj, S. Petrides, and L. F. Demkowicz. Construction of DPG Fortin operators for second order problems. *Computers & Mathematics with Applications*, 74(8):1964–1980, 2017.

[35] S. Petrides and L. F. Demkowicz. An adaptive DPG method for high frequency time-harmonic wave propagation problems. *Computers & Mathematics with Applications*, 74(8):1999–2017, 2017.

[36] N. V. Roberts and S. Henneking. Time-stepping DPG formulations for the heat equation. *Computers & Mathematics with Applications*, 95:242–255, 2021.

[37] S. Rojas, D. Pardo, P. Behnoudfar, and V. M. Calo. Goal-oriented adaptivity for a conforming residual minimization method in a dual discontinuous Galerkin norm. *Computer Methods in Applied Mechanics and Engineering*, 377:113686, 2021.

[38] E. Valseth and C. Dawson. An unconditionally stable space–time FE method for the Korteweg–de Vries equation. *Computer Methods in Applied Mechanics and Engineering*, 371:113297, 2020.

[39] E. Valseth, A. Romkes, and A. R. Kaul. A stable FE method for the space-time solution of the Cahn-Hilliard equation. *Journal of Computational Physics*, 441:110426, 2021.